Deterministic Particle Methods for High Dimensional Fokker-Planck Equations

M. Junk[1] and G. Venkiteswaran[2]

[1] Fachbereich Mathematik und Statistik, Fach D194, Universität Konstanz
michael.junk@uni-konstanz.de
[2] Department of Mathematics, Birla Institute of Technology and Science, Vidya Vihar Campus Pilani 333 031 Rajasthan, India gvenki@bits-pilani.ac.in

Summary. We consider a mathematical model for polymeric liquids which requires the solution of high-dimensional Fokker-Planck equations related to stochastic differential equations. While Monte-Carlo (MC) methods are classically used to construct approximate solutions in this context, we consider an approach based on Quasi-Monte-Carlo (QMC) approximations. Although QMC has proved to be superior to MC in certain integration problems, the advantages are not as pronounced when dealing with stochastic differential equations. In this article, we illustrate the basic difficulty which is related to the construction of QMC product measures.

Key words: QMC, Fokker-Planck equation, stochastic differential equation, product measures

1 A polymer model

In order to understand the non-Newtonian behavior of polymeric liquids (see [1] for a list of phenomena), various polymer models have been investigated in the literature. Here, we consider the so called Rouse chain model [2], in which sub-strings of the polymer molecules are represented by beads (see figure 1) and interactions are indicated by connecting springs (even though a more complicated interaction potential is employed, as specified below). The geometrical configuration of such a chain is described by specifying all the connector vectors $\boldsymbol{Q}_i := \boldsymbol{r}_{i+1} - \boldsymbol{r}_i$, $i = 1, \ldots, n-1$, where $\boldsymbol{r}_\nu$, $\nu = 1, \ldots, n$ are the position vectors of the beads. Since each of the vectors $\boldsymbol{Q}_i$ has three components, the configuration space is $\mathbb{R}^s$ with $s = 3(n-1)$. For example, a chain with $n = 30$ beads requires $s = 87$ numbers to describe its geometrical configuration. We assume that many such bead-spring chains are immersed into a solvent liquid which undergoes a linear flow, for example a shear flow with velocity field

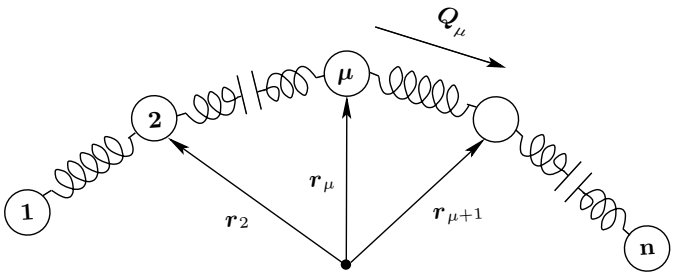

Figure 1. Rouse model of a bead-spring chain.

$$\boldsymbol{v}(\mathbf{x}) = \boldsymbol{\kappa}\,\mathbf{x}, \qquad \boldsymbol{\kappa}{:=}\beta \begin{pmatrix} 0 & 1 & 0 \\ 0 & 0 & 0 \\ 0 & 0 & 0 \end{pmatrix},$$

where β is the constant shear rate. The solvent is considered to exert a drag force, and a random Brownian force on the chain, and the chain is considered to interact with itself through a potential which consists of two contributions, a quadratic attractive part that prevents the beads of the chain from going very far apart, and a Gaussian repulsive part called the excluded volume potential [10], that resists any pair of beads from coming very close to each other. In the following, we list the momentum increment due to the various forces.

Potential force

The momentum increase of bead ν due to potential forces is given by

$$d\boldsymbol{p}_\nu^{(\phi)}{:=} -\frac{\partial \phi}{\partial \boldsymbol{r}_\nu}\,dt, \tag{1}$$

where

$$\phi{:=}\frac{1}{2}\sum_i H\mathbf{Q}_i\cdot\mathbf{Q}_i + k_BT\,\frac{z}{d^3}\sum_{\substack{\mu,\nu=1\\ \mu\neq\nu}}^{n}\exp\left(-\frac{H}{k_BT}\,\frac{r_{\mu\nu}^2}{2d^2}\right).$$

Here, H is the spring constant of the attractive part, T is the solvent temperature, k_B is Boltzmann's constant, $r_{\mu\nu}$ is the magnitude of the vector $\boldsymbol{r}_{\mu\nu}{:=}\boldsymbol{r}_\mu - \boldsymbol{r}_\nu$, connecting the pair of beads μ and ν, the parameter d controls the extent of the repulsive potential, and z describes its strength.

Hydrodynamic drag force

This is the force of resistance the bead experiences as it moves through the solvent. Under the assumption that the beads are spherical in shape, an expression for this force can be written using Stokes' law as

$$\boldsymbol{F}_\nu^{(h)} = -\xi\cdot(\dot{\boldsymbol{r}}_\nu - \boldsymbol{v}(\boldsymbol{r}_\nu)).$$

According to this law, the force on bead ν is directly proportional to the difference between the bead velocity $\dot{\boldsymbol{r}}_\nu$ and the velocity of the solution $\boldsymbol{v}(\boldsymbol{r}_\nu)$ at bead ν. The parameter ξ is the Stokes' friction coefficient. The corresponding momentum increment is

$$d\boldsymbol{p}_\nu^{(h)} := \boldsymbol{F}_\nu^{(h)}\, dt = -\xi \cdot (d\boldsymbol{r}_\nu - \boldsymbol{v}(\boldsymbol{r}_\nu)\, dt).$$

Brownian force

Due to the thermal fluctuations of the solvent molecules, the bead experiences a random force and this force is modeled by a Wiener process. The momentum changes are thus given by

$$d\boldsymbol{p}_\nu^{(b)} := \sqrt{2k_BT\xi}\, d\boldsymbol{W}_\nu$$

where $\boldsymbol{W}_\nu$ are independent three dimensional Wiener processes. The factor $\sqrt{2k_BT\xi}$ signifies the fact that the energy of the solvent molecules is due to the temperature of the solvent, T, and this energy influences the collision with the beads.

Force balance

In our force balance, we neglect interaction between different chains which amounts to the implicit assumption of a dilute polymeric solution. Also, the hydrodynamic interaction between the beads will be neglected, i.e. we assume that the flow field is given by $\boldsymbol{v}$, even though the presence of the beads leads to local perturbations. Finally, we assume that inertia forces play a negligible role in the process. Altogether, the force balance

$$d\boldsymbol{p}_\nu^{(\phi)} + d\boldsymbol{p}_\nu^{(h)} + d\boldsymbol{p}_\nu^{(b)} = 0$$

gives rise to a system of first order stochastic differential equations

$$d\boldsymbol{r}_\nu = \left[\boldsymbol{v}(\boldsymbol{r}_\nu) - \frac{1}{\xi}\frac{\partial \phi}{\partial \boldsymbol{r}_\nu}\right] dt + \sqrt{\frac{2k_BT}{\xi}}\, d\mathbf{W}_\nu, \qquad \nu = 1.\ldots, n.$$

Using the linear relation between the bead position vectors $\boldsymbol{r}_\nu$ and the connector vectors

$$\boldsymbol{Q}_k = \sum_\nu \bar{B}_{k\nu}\boldsymbol{r}_\nu, \qquad \bar{B}_{k\nu} = \delta_{k+1,\nu} - \delta_{k,\nu}$$

the system can be reformulated with $A = \bar{B}\bar{B}^T$ (see [12] for details)

$$d\boldsymbol{Q}_j = \left[\boldsymbol{v}(\boldsymbol{Q}_j) - \frac{1}{\xi}\sum_k A_{jk}\frac{\partial \phi}{\partial \boldsymbol{Q}_k}\right] dt + \sqrt{\frac{2k_BT}{\xi}}\, \left[\sum_\nu \bar{B}_{j\nu}\, d\mathbf{W}_\nu\right],\ j = 1, \ldots, n-1.$$

Combining all connector vectors to a single $\mathbb{R}^s$-vector $\boldsymbol{Q}$ and introducing obvious abbreviations, the system can be written in the compact form

$$d\boldsymbol{Q} = \boldsymbol{a}(\boldsymbol{Q})\, dt + D\, d\boldsymbol{W}. \tag{2}$$

Associated Fokker-Planck equation

Assuming that the Itô process $\boldsymbol{Q}$ is a solution of (2) such that $\boldsymbol{Q}(t)$ possesses, for each $t \geq 0$, a smooth Lebesgue-density $\psi(t, \boldsymbol{q})$, we show formally, that ψ is a solution of a Fokker-Planck equation on $\mathbb{R}^s$. To this end, take any test function $f : [0, \infty) \times \mathbb{R}^s \to \mathbb{R}$. Itô's formula [5] implies (with summation convention for the indices i, j, k running from 1 to s)

$$f(t, \boldsymbol{Q}(t)) = f(0, \boldsymbol{Q}(0)) + \int_0^t D_{ij} \frac{\partial f}{\partial q_i}(s, \boldsymbol{Q}(s))\, dW_j(s) + \int_0^t \left(\frac{\partial f}{\partial t} + a_i \frac{\partial f}{\partial q_i} + \frac{1}{2} D_{ik} D_{jk} \frac{\partial^2 f}{\partial q_i \partial q_j} \right)(s, \boldsymbol{Q}(s))\, ds.$$

Computing the expected value of $f(t, \boldsymbol{Q}(t))$ using the density of $\boldsymbol{Q}(t)$ and noting that the expected value of the stochastic integral vanishes, we obtain

$$\int_{\mathbb{R}^s} f(t, \boldsymbol{q}) \psi(t, \boldsymbol{q})\, d\boldsymbol{q} = \int_{\mathbb{R}^s} f(0, \boldsymbol{q}) \psi(0, \boldsymbol{q})\, d\boldsymbol{q} + \int_{\mathbb{R}^s} \int_0^t \left(\frac{\partial f}{\partial t} + a_i \frac{\partial f}{\partial q_i} + \frac{1}{2} D_{ik} D_{jk} \frac{\partial^2 f}{\partial q_i \partial q_j} \right)(s, \boldsymbol{q}) \psi(s, \boldsymbol{q})\, ds\, d\boldsymbol{q}.$$

Integration by parts allows us to move the derivatives over to the density

$$\int_{\mathbb{R}^s} \int_0^t \left(\frac{\partial \psi}{\partial t} + \frac{\partial}{\partial q_i}(a_i \psi) - \frac{1}{2} D_{ik} D_{jk} \frac{\partial^2 \psi}{\partial q_i \partial q_j} \right)(s, \boldsymbol{q}) f(s, \boldsymbol{q})\, ds\, d\boldsymbol{q} = 0$$

and since f was an arbitrary test function, we see that ψ is a solution of the Fokker-Planck equation

$$\frac{\partial \psi}{\partial t} + \frac{\partial}{\partial q_i}(a_i \psi) = \frac{1}{2} D_{ik} D_{jk} \frac{\partial^2 \psi}{\partial q_i \partial q_j}$$

depending on the high-dimensional variable $\boldsymbol{q} = (q_1, \ldots, q_s) \in \mathbb{R}^s$. In our particular case, the equation has the form

$$\frac{\partial\, \psi}{\partial t} = -\sum_{j=1}^{n-1} \frac{\partial}{\partial \boldsymbol{Q}_j} \cdot \left(\boldsymbol{\kappa}\, \boldsymbol{Q}_j - \frac{1}{4} \sum_{k=1}^{n-1} A_{jk} \frac{\partial \phi}{\partial \boldsymbol{Q}_k} \right) \psi + \frac{1}{4} \sum_{j,\, k=1}^{n-1} A_{jk} \frac{\partial}{\partial \boldsymbol{Q}_j} \cdot \frac{\partial \psi}{\partial \boldsymbol{Q}_k}$$

where, $\partial / \partial \boldsymbol{Q}_j \cdot$ denotes divergence with respect to $\boldsymbol{Q}_j$ and $\partial \psi / \partial \boldsymbol{Q}_k$ the $\boldsymbol{Q}_k$ gradient.

The target quantity

The quantity we are ultimately interested in is the stress tensor $\boldsymbol{\tau}^s + \boldsymbol{\tau}^p$ which characterizes the flow behavior of polymeric liquids. It consists of two contributions namely, one from the solvent $\boldsymbol{\tau}^s$, and the other from the polymer

$\boldsymbol{\tau}^p$. The rheological properties of the polymer solution can be obtained by calculating the polymer contribution to the stress tensor, which is given by Kramers expression [2],

$$\boldsymbol{\tau}^p := \int_{\mathbb{R}^s} \Gamma(\boldsymbol{q})\psi_\infty(\boldsymbol{q})\, d\boldsymbol{q}, \qquad \Gamma(\boldsymbol{q}) := -\sum_{j=1}^{n-1} \boldsymbol{q}_j \otimes \frac{\partial \phi}{\partial \boldsymbol{q}_j}(\boldsymbol{q}). \tag{3}$$

where ψ_∞ is the stationary solution of the Fokker-Planck equation.

Mathematical problem

In view of the above, the mathematical task can be summarized as follows. We have to solve a system of s stochastic differential equations

$$d\boldsymbol{Q} = \boldsymbol{a}(\boldsymbol{Q})\, dt + D\, d\boldsymbol{W}, \qquad \boldsymbol{Q}(0) = \boldsymbol{Q}_0 \tag{4}$$

and compute the expected value $E(\Gamma(\boldsymbol{Q}(t)))$ for $t \to \infty$. Equivalently, we can solve the Fokker-Planck initial value problem on $\mathbb{R}^s$

$$\frac{\partial \psi}{\partial t} + \frac{\partial}{\partial q_i}(a_i \psi) = \frac{1}{2} D_{ik} D_{jk} \frac{\partial^2 \psi}{\partial q_i \partial q_j}, \qquad \psi|_{t=0} = \psi_0 \tag{5}$$

for the density corresponding to $\boldsymbol{Q}$ and compute, for large t,

$$\boldsymbol{\tau}(t) = \int_{\mathbb{R}^s} \Gamma(\boldsymbol{q})\psi(t, \boldsymbol{q})\, d\boldsymbol{q}. \tag{6}$$

Model problem

To develop ideas, we study an important but simplified version of problem (4) resp. (5) where the deterministic part $\boldsymbol{a}$ is set to zero. Specifically, we consider a system of s stochastic differential equations

$$d\boldsymbol{z}_t = d\boldsymbol{W}_t, \qquad \boldsymbol{z}_0 = 0 \tag{7}$$

with associated Fokker-Planck equation

$$\frac{\partial u}{\partial t} = \frac{1}{2} \Delta u, \qquad u|_{t=0} = \delta_0 \tag{8}$$

which is the diffusion equation with Dirac-delta initial value. The target value is assumed to be of the form

$$\mu_t = E(g(\boldsymbol{z}_t)) = \int_{\mathbb{R}^s} g(\boldsymbol{y}) u(t, \boldsymbol{y})\, d\boldsymbol{y} \tag{9}$$

where g is some given function which generalizes Γ in (6).

2 Meshfree solution methods

Due to the high dimension of the configuration space $\mathbb{R}^s$, traditional methods like quadrature rules, finite differences or finite elements, are not useful for the discretization of integral functionals of type (9) or parabolic equations like (5) or (8). Indeed, the number of node points needed to achieve a prescribed accuracy with these methods grows exponentially with the dimension which is referred to as the curse of dimension [9]. The famous approach which breaks this curse is the Monte Carlo (MC) method. In our context, it is used to approximately evaluate the integral (9) and to solve (7). Using MC integration, we obtain

$$\mu_T = E(g(\boldsymbol{z}_T)) \approx \frac{1}{N}\sum_{i=1}^{N} g(\tilde{\boldsymbol{z}}_T(i)) \tag{10}$$

provided $\tilde{\boldsymbol{z}}_T(1), \tilde{\boldsymbol{z}}_T(2), \dots$ are independent pseudo random vectors which are distributed approximately like the solution $\boldsymbol{z}_T$ of (7). Such vectors can be obtained, for example, with the Euler-Maruyama MC method [5]. This straight forward solution algorithm is based on replacing the differentials d in (7) with corresponding time differences. Introducing a regular time discretization $t_m = mh$ with $m \in \mathbb{N}_0$, the Wiener increments $\boldsymbol{W}_{t_{m+1}} - \boldsymbol{W}_{t_m}$ are normal distributed with variance equal to the time increment $t_{m+1} - t_m = h$. If $\tilde{\boldsymbol{y}}_{t_m}(1), \tilde{\boldsymbol{y}}_{t_m}(2), \dots$ are independent pseudo random vectors with the same distribution as the Wiener increments, the Euler-Maruyama method for (7) reads

$$\tilde{\boldsymbol{z}}_{t_{m+1}(i)} = \tilde{\boldsymbol{z}}_{t_m}(i) + \tilde{\boldsymbol{y}}_{t_m}(i), \quad \tilde{\boldsymbol{z}}_0(i) = 0, \qquad i = 1, \dots, N. \tag{11}$$

An alternative to the classical MC methods described above is given by Quasi-Monte-Carlo (QMC) methods which are in the focus of this article. Particularly for the integration problem, QMC methods have shown to be superior to the MC approach under certain assumptions on the integrand. While the QMC integral approximation also has the form (10), the pseudo random vectors $\tilde{\boldsymbol{z}}_T(i)$ are replaced by points $\boldsymbol{Z}_T(1), \dots, \boldsymbol{Z}_T(N) \in \mathbb{R}^s$ with different properties. To obtain a good approximation by

$$\frac{1}{N}\sum_{i=1}^{N} g(\boldsymbol{Z}_T(i)) \approx E(g(\boldsymbol{z}_T)) = \int_{\mathbb{R}^s} g(\boldsymbol{y}) u(T, \boldsymbol{y})\, d\boldsymbol{y},$$

the points $\boldsymbol{Z}_T(i)$ should be constructed in such a way that the associated point measure

$$\Pi_{\boldsymbol{Z}_T} := \frac{1}{N}\sum_{i=1}^{N} \delta_{\boldsymbol{Z}_T(i)}$$

is a good approximation of the measure $u(t, \boldsymbol{y})\, d\boldsymbol{y}$. The approximation error is quantified deterministically in terms of the *discrepancy* between the two measures (for details, see [8] and the following section) which is an advantage compared to MC methods where the quality of the pseudo random vectors is

checked with less reliable statistical tests. On the other hand, the basic MC concept of *independence* is typically *not* available in the QMC context which turns out to be a drawback in the construction of the measure approximation $\Pi_{\boldsymbol{Z}_T}$. Following [6, 14], for example, the required points $\boldsymbol{Z}_T(i)$ are constructed from a measure approximation of the solution to (8) which uses the integral representation in terms of the fundamental solution. The final algorithm has a form similar to the Euler-Maruyama method (11)

$$\boldsymbol{Z}_{t_{m+1}}(i) = \boldsymbol{Z}_{t_m}(i) + \boldsymbol{Y}_{t_m}(P(i)), \quad \boldsymbol{Z}_0(i) = 0, \qquad i = 1, \ldots, N. \tag{12}$$

In this recursion formula, the vectors $\boldsymbol{Y}_{t_m}(1), \ldots, \boldsymbol{Y}_{t_m}(N)$ should constitute a point measure approximation $\Pi_{\boldsymbol{Y}_{t_m}}$ of the measure $G_h(\boldsymbol{y})\, d\boldsymbol{y}$ related to the fundamental solution

$$G_h(\boldsymbol{y}) := \frac{1}{(4\pi h)^{s/2}} \exp\left(-\frac{|\boldsymbol{y}|^2}{4h}\right), \quad \boldsymbol{y} \in \mathbb{R}^s \tag{13}$$

of the diffusion equation at time $h > 0$. Note that this requirement parallels the assumption on the pseudo random vectors $\tilde{\boldsymbol{y}}_{t_m}(i)$ in (11) which must be normal distributed with the same density (13). Also the *independence* of the increments $\tilde{\boldsymbol{y}}_{t_m}(i)$ from the states $\tilde{\boldsymbol{z}}_{t_m}(i)$ has its parallel in the QMC algorithm. To explain this point, we recall that independence of $\tilde{\boldsymbol{y}}_{t_m}(i)$ and $\tilde{\boldsymbol{z}}_{t_m}(i)$ is equivalent to the condition that the distribution of the pairs $(\tilde{\boldsymbol{z}}_{t_m}(i), \tilde{\boldsymbol{y}}_{t_m}(i)) \in \mathbb{R}^{2s}$ is the *product* of the separate distributions. In view of this, it is not surprising that the permutation $P : \{1, \ldots, N\} \to \{1, \ldots, N\}$ in (12) has to ensure that the pairs $(\boldsymbol{Z}_{t_m}(i), \boldsymbol{Y}_{t_m}(P(i))) \in \mathbb{R}^{2s}$ give rise to a point measure approximation of the *product measure* $\Pi_{\boldsymbol{Z}_{t_m}} \otimes \Pi_{\boldsymbol{Y}_{t_m}}$.

The two requirements on the increments $\boldsymbol{Y}_{t_m}(P(1)), \ldots, \boldsymbol{Y}_{t_m}(P(N))$ to be correctly distributed according to (13) and to be suitably independent from the vectors $\boldsymbol{Z}_{t_m}(1), \ldots, \boldsymbol{Z}_{t_m}(N)$ are essential in the derivation presented in [6, 14]. Obviously, the main difference to the MC approach is the required construction of the permutation P to ensure independence, or equivalently, to ensure the product measure approximation. Unfortunately, this crucial construction is both time consuming (P involves high-dimensional sorting and quasi-random mixing) and unfavorable for the accuracy of the QMC approach. In fact, the discrepancy estimate given in [6] indicates a convergence order well below $\sqrt{N}$ in high dimensions, although in practice, the QMC approach is still somewhat more accurate than the MC version.

A similar observation has been made in [13], and in [14], where the importance of sorting the QMC points before adding the increments $\boldsymbol{Y}_{t_m}(i)$ has been demonstrated experimentally. Similarly, in [7], the role of sorting the QMC points is highlighted.

These observations have motivated us to take a closer look at the important question, how to construct product measures from given QMC point sets.

3 QMC product measures

In this section, we study the fundamental problem how to construct a point measure approximation of the Lebesgue measure on the s dimensional unit cube from two lower dimensional point measure approximations. Our construction is guided by a discrepancy estimate for the resulting product measure in terms of the two participating measures. The discussion in the previous section suggests that changing the numbering of the QMC points (using permutations) plays an important role in the construction. This will also become obvious from the results below.

To introduce the relevant concepts, we first define generalized intervals $[\boldsymbol{a},\boldsymbol{b})$ with $\boldsymbol{a},\boldsymbol{b}\in\mathbb{R}^s$ according to

$$[\boldsymbol{a},\boldsymbol{b}):=\prod_{i=1}^{s}[a_i,b_i).$$

If $\mathbf{0}$ denotes the zero vector and $\mathbf{1}$ the vector having a one in each component, the s-dimensional unit cube I^s can be written in the form $I^s=[\mathbf{0},\mathbf{1})$. The set of all sub intervals $[\mathbf{0},\boldsymbol{u})$, $\boldsymbol{u}\in I^s$ of the unit interval with $\mathbf{0}$ as a corner is denoted $\mathcal{R}_s^*$.

Since we restrict our attention to point measures with equal weights, it suffices to specify the point locations to uniquely define the measure. Hence, a point measure on I^s is characterized by a mapping $X:\mathcal{N}\to I^s$ on a finite index set $\mathcal{N}=\{1,\dots,N\}$. We will employ the usual notation $X\in J$ resp. $\{X\in J\}$ to denote the set of indices $\{i\in\mathcal{N}\,:\,X(i)\in J\}$. If Cnt is the counting measure, $\delta_{X(i)}$ the Dirac measure located at $X(i)$, and $\mathcal{B}$ the family of Borel sets in I^s, the point measure associated to X is defined by

$$\Pi_X(J):=\frac{1}{N}\sum_{i=1}^{N}\delta_{X(i)}(J)=\frac{\mathrm{Cnt}(X\in J)}{\mathrm{Cnt}(X\in I^s)},\qquad J\in\mathcal{B}.$$

Notice that Π_X is invariant under permutations, i.e. $\Pi_X=\Pi_{X\circ P}$ for every permutation $P:\mathcal{N}\to\mathcal{N}$.

The point measure of a set J approximates its s-dimensional Lebesgue measure $\lambda_s(J)$ if the difference

$$\Delta(X,J):=|\Pi_X(J)-\lambda_s(J)|$$

is small. If $\Delta(X,J)$ is small for *all* intervals $J\in\mathcal{R}_s^*$, then the point measure is a good approximation of the Lebesgue measure. The approximation quality can be measured with the star-discrepancy of X

$$D^*(X):=\sup_{J\in\mathcal{R}_s^*}\Delta(X,J).$$

Since Π_X is invariant under renumbering, we conclude that also the discrepancy satisfies $D^*(X)=D^*(X\circ P)$ for every permutation $P:\mathcal{N}\to\mathcal{N}$.

The problem we address is the following: Assume X_1, X_2 are two functions from $\mathcal{N}$ into the unit cubes I^{s_1} respectively I^{s_2} and assume we have some information about the discrepancies $D^*(X_1)$ and $D^*(X_2)$. What can we say about the discrepancy $D^*(X)$ of the measure defined by $X = (X_1, X_2)$ on the product cube I^s, $s = s_1 + s_2$?

The special case $X_2 = X_1$ immediately shows that the quality of the product measure may be arbitrarily bad unless we specify further conditions on X_1 and X_2 (in the case $X_2 = X_1$ all points will be on the s_1-dimensional diagonal in the $2s_1$-dimensional product cube, which is far from the Lebesgue measure, even if X_1 has a very small star-discrepancy).

Our assumptions are motivated by the observation that low discrepancy point sets $\{X_2(1), \ldots, X_2(N)\}$ can be constructed with a discrepancy estimate of the form

$$D^*(X_2) \leq \frac{l_2(N)}{N}, \qquad N = \mathrm{Cnt}(X_2 \in I^{s_2}) \tag{14}$$

where $l_2(N)$ is of the form $c \log^s(N)$ with some constant $c > 0$. However, our estimates will only use that l_2 is a non-negative and non-decreasing function.

Our assumptions on X_1 are a generalization of the situation which arises if we take $X_1(1), \ldots, X_1(N)$ as the first N points of a Faure sequence [3]. This low discrepancy *sequence* $\boldsymbol{y}_1, \boldsymbol{y}_2, \ldots$ has the property that any consecutive subset $\boldsymbol{y}_{k+1}, \boldsymbol{y}_{k+2}, \ldots, \boldsymbol{y}_{k+m}$ gives rise to a point measure with a discrepancy estimate depending only on the length m of the subset and *not* on the starting index $k + 1$. The estimate is again of the form $l_1(m)/m$ with a logarithmic factor l_1. To state our assumptions more precisely, we need

Definition 1. *A finite set $A \subset \mathbb{N}$ is called consecutive if it contains all $n \in \mathbb{N}$ between* $\min A$ *and* $\max A$.

Then we assume that

$$D^*(X_1|_C) \leq \frac{l_1(m)}{m}, \quad m = \mathrm{Cnt}(C),\ C \subset \mathcal{N} \text{ consecutive} \tag{15}$$

where l_1 is a non-negative and non-decreasing function.

In order to formulate our main discrepancy estimate, we now introduce a concept which eventually demonstrates why and how the numbering of the points $X_2(1), \ldots, X_2(N)$ affects the quality of the product measure. To explain the idea, let us take some interval $J_2 \in \mathcal{R}^*_{s_2}$ and assume that the associated index set $\{X_2 \in J_2\}$ has the form

$$\{X_2 \in J_2\} = \{12, 13, 25, 28, 29, 30\}.$$

This set has several *consecutive representations*, for example

$$\{12, 13, 25, 28, 29, 30\} = \{12\} \cup \{13\} \cup \{25\} \cup \{28\} \cup \{29, 30\},$$

but only one *smallest* representation

$$\{12, 13, 25, 28, 29, 30\} = \{12, 13\} \cup \{25\} \cup \{28, 29, 30\},$$

with $\mathrm{cc}(X_2 \in J_2) = 3$ connected components. In this way, we can associate to each interval J_2 the number $\mathrm{cc}(X_2 \in J_2)$ of connected components and the largest number that appears in this process is denoted $\mathrm{cc}^*(X_2)$. It should be clear that this value depends on the numbering, i.e. we typically have $\mathrm{cc}^*(X_2) \neq \mathrm{cc}^*(X_2 \circ P)$ if $P : \mathcal{N} \to \mathcal{N}$ is a permutation.

In general, it is clear that if A and A' are consecutive and if $A \cap A' \neq \emptyset$ then $A \cup A'$ is also consecutive. Using this observation, we can conclude that, for every finite set $A \subset \mathbb{N}$, there exists a *unique* smallest consecutive representation of pairwise disjoint consecutive sets (if the sets were not pairwise disjoint, one could merge at least two of them violating the minimality; if there was a different representation with the same number of sets, at least one of them would intersect two other sets of the original representation which again violates minimality). This observation allows us to state

Definition 2. *The sets of the smallest consecutive representation of a finite set $A \subset \mathbb{N}$ are called consecutive components. The number of consecutive components is denoted* $\mathrm{cc}(A)$. *For $X_2 : \{1, \ldots, N\} \to I^{s_2}$ with $N, s_2 \in \mathbb{N}$ we denote*

$$\mathrm{cc}^*(X_2) := \sup_{J_2 \in \mathcal{R}^*_{s_2}} \mathrm{cc}(X_2 \in J_2).$$

The proof of the following main result can be found in [4].

Theorem 1. *Let $X_i : \mathcal{N} \to I^{s_i}$, $i = 1, 2$ be mappings from $\mathcal{N} = \{1, \ldots, N\}$ into the unit cubes I^{s_1} and I^{s_2} with $N, s_1, s_2 \in \mathbb{N}$ which satisfy* (14) *and* (15). *Then the star-discrepancy of $X = (X_1, X_2)$ can be estimated by*

$$D^*(X) \leq \frac{l_2(N)}{N} + \mathrm{cc}^*(X_2) \frac{l_1(N)}{N}.$$

Obviously, the discrepancy estimate of Theorem 1 is optimal, if the worst number of consecutive components $\mathrm{cc}^*(X_2)$ is as small as possible. Since $\mathrm{cc}^*(X_2)$ depends on the numbering of the points, it is also clear that a suitable permutation of the point numbers may improve the quality of the product measure.

3.1 The one-dimensional case

To illustrate the role of sorting in the construction of product measures the case $s_2 = 1$ is most enlightening.

For example, if $X_2(1), \ldots, X_2(N)$ are the first N members of the Sobol sequence [11]

$$0\,, \frac{1}{2}\,, \frac{1}{4}\,, \frac{3}{4}\,, \frac{3}{8}\,, \frac{7}{8}\,, \frac{1}{8}\,, \frac{5}{8}\,, \frac{5}{16}\,, \frac{13}{16}\,, \ldots$$

we find for $J_2 = [0, 1/2)$ and $N = 10$

$$\{X_2 \in J_2\} = \{1, 3, 5, 7, 9\}$$

so that the number of consecutive components is $\mathrm{cc}(X_2 \in J_2) = 5 = N/2$. A similar behavior is observed for larger N in the case $J_2 = [0, 1/2)$, i.e. the number $\mathrm{cc}(X_2 \in J_2)$ of consecutive subsets is essentially $N/2$ which ruins the estimate of Theorem 1.

However, if we *sort* the leading N values of the Sobol sequence before assigning them as values of X_2, the situation is much better. In our example above, the sorted values are

$$0\,,\ \frac{1}{8}\,,\ \frac{1}{4}\,,\ \frac{5}{16}\,,\ \frac{3}{8}\,,\ \frac{1}{2}\,,\ \frac{5}{8}\,,\ \frac{3}{4}\,,\ \frac{13}{16}\,,\ \frac{7}{8}$$

so that

$$\{X_2 \in J_2\} = \{1, 2, 3, 4, 5\}$$

which is consecutive, i.e. $cc(X_2 \in J_2) = 1$. More generally, if the points $X_2(1), \ldots, X_2(N)$ are sorted, or in other words if X_2 is a monotone function, we can find for each $J_2 = [0, u_2)$ a unique index m such that

$$\{X_2 \in J_2\} = \{1, \ldots, m\}.$$

and hence $\mathrm{cc}^*(X_2 \in J_2) = 1$. Using Theorem 1, we conclude

Corollary 1. *Let X_2 be an increasing mapping from $\mathcal{N} = \{1, \ldots, N\}$, $N \in \mathbb{N}$ to the unit interval I with a discrepancy estimate of the form* (14)*. Assume further that $X_1 : \mathcal{N} \to I^{s_1}$ satisfies* (15)*. Then the discrepancy of $X = (X_1, X_2)$ can be estimated by*

$$D^*(X) \le \frac{l_1(N) + l_2(N)}{N}.$$

We remark that this result parallels the case mentioned in [14] where the case $s_1 = s_2 = 1$ has been considered with a slightly weaker assumption on the points X_1.

3.2 The general case

We describe the two-dimensional case $s_2 = 2$ to explain the effect of sorting in higher dimensional situations.

To give a first example, we consider $N = 16$ points of the two-dimensional Halton sequence with bases two and three. If we connect consecutive points with lines, the curve on the left of figure 2 appears. Given an interval of the form $J_2 = [\mathbf{0}, \boldsymbol{u}_2)$, the consecutive components of $\{X_2 \in J_2\}$ can then be visualized in the following way: as before, we connect consecutive points but now only as long as they are in J_2. Whenever a node $X_2(i) \in J_2$ has a successor outside J_2, the curve terminates at $X_2(i)$ and a new curve is started at the smallest index $j > i$ for which again $X_2(j) \in J_2$. Each snippet obtained in this way is a connected subset of the original curve and corresponds directly to a consecutive component of $\{X_2 \in J_2\}$. For our example above, the snippets corresponding to $\boldsymbol{u}_2 = \left(\begin{smallmatrix} 0.8 \\ 0.7 \end{smallmatrix}\right)$ are visualized on the right of figure 2.

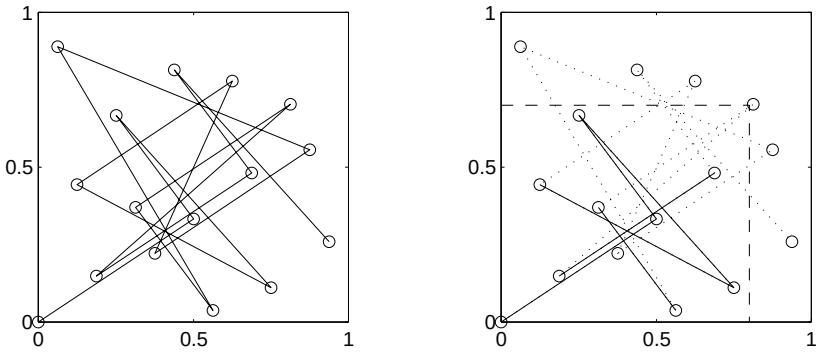

Figure 2. Left: the first 16 points of the Halton sequence with bases two and three connected in the order of appearance. Right: the interval J_2 is indicated by the dashed line and the four consecutive subsets of $\{X_2 \in J_2\}$ are represented by solid lines. The snippets of the original curve correspond to the consecutive index sets $\{1,\ldots,5\},\{7\},\{10,11\},\{13,14\}$.

From these considerations it should intuitively be clear that a very irregular curve is generally cut into more snippets by intersection with intervals than a more regular curve. The idea is therefore to keep the node locations which assure the required low discrepancy of X_2 but to connect them in a different order, resulting in a more regular curve which leads to less snippets when cut with an interval. In other words, if $\tilde{X}_2 : \mathcal{N} \to I^2$ refers to the original node distribution, we try to construct a permutation $P : \mathcal{N} \to \mathcal{N}$ such that $X_2 = \tilde{X}_2 \circ P$ gives rise to a better behavior.

Again, this can be achieved by a suitable sorting. To this end, we choose some $m \in \mathbb{N}$, split the unit square into m equal sized columns (m-bins)

$$B_k := \big[\frac{k}{m}, \frac{k+1}{m}\big) \times \big[0,1\big), \qquad k = 0,\ldots,m-1$$

and sort the points in each bin separately with respect to the last component. Similarly, in the general case, m-bins are sub-intervals which have side length $1/m$ in the first s_2-1 directions and length 1 in direction s_2. Sorting is carried out in each bin with respect to the last component. Connecting the sorted subsets according to the bin numbers, we obtain a new global numbering of the points. In our previous example, the corresponding curve is visualized in figure 3 for the case $m = 4$. Of course, there are many other ways to connect the given nodes with reasonable curves. Some more examples are presented and analyzed in [4].

Using Theorem 1, we can prove that sorting in m-bins allows to produce reasonable QMC product measures, by estimating $\mathrm{cc}^*(X_2)$. In other words, we have to find an upper bound for the number of consecutive components of sets $\{X_2 \in J\}$ with $J = [\mathbf{0}, \boldsymbol{u})$ and $\boldsymbol{u} \in I^{s_2}$. We develop the idea in the case $s_2 = 2$ and refer to [4] for a rigorous investigation. The idea of the estimate

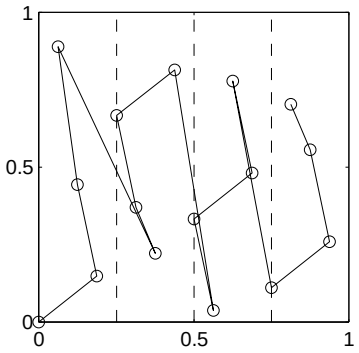

Figure 3. The first 16 points of the Halton sequence with bases two and three connected according to the numbering which follows from sorting the second coordinate in each bin separately (the bins are indicated by vertical dashed lines).

is the following: if k is the number of the bin which contains $\boldsymbol{u}$, all the bins to the left of bin B_k are cut by J. In each of these bins B_i, the intersection $J \cap B_i$ contains not more than one consecutive component. Hence, the number of consecutive components related to $J \cap B$ with $B = \cup_{i=1}^{k-1} B_i$ is bounded by $k \leq m$ (respectively by m^{s_2-1} in the general case so that m should not be too large). In the remaining set $J \backslash B$ we could face the worst case that the curve connecting the points is zig-zagging around the vertical line through u_1. This would give rise to many single-point components (essentially half the number of points contained in $J \backslash B$). Hence, m should be as large as possible because small bins contain fewer points. A *balanced* estimate is obtained if m is chosen of the order of $N^{\frac{1}{s_2}}$. For the two-dimensional case, this is easy to see because each of the $m = \sqrt{N}$ bins contains essentially $N/m = \sqrt{N}$ points if the points are uniformly distributed, i.e. if the discrepancy of the point set is reasonably small. Hence the number of consecutive components can be estimated by $\mathrm{cc}^*(X_2) \leq m + N/m = O(\sqrt{N})$. A careful version of this argument is given in [4] which proves

Theorem 2. *Let $X_i : \mathcal{N} \to I^{s_i}$, $i = 1, 2$ be mappings from $\mathcal{N} = \{1, \ldots, N\}$ into the unit cubes I^{s_1} and I^{s_2} with $N, s_1, s_2 \in \mathbb{N}$. Assume further that X_1, X_2 satisfy* (14) *and* (15) *and that that the points $X_2(i)$ are sorted in m-bins with $m = \lfloor N^{\frac{1}{s_2}} \rfloor + 1$. Then the star-discrepancy of $X = (X_1, X_2)$ satisfies*

$$D^*(X) \leq \frac{l_1(N)(1+s_2)}{N^{\frac{1}{s_2}}} + \frac{l_2(N)(1+2l_1(N))}{N}.$$

In summary, we can say that sorting plays an essential role in the construction of QMC product measures. The obtained discrepancy estimate, however, is quite poor in high dimensions. Among other things, this is due to the fact that we estimate the worst case error which may not play a big role in specific applications. Therefore, numerical investigations are necessary to judge about

the practical usefulness of the QMC approach. In the following section, such questions are addressed.

4 QMC simulations

4.1 The diffusion equation

In order to construct approximate solutions of the model problem (8), we use a QMC algorithm of the form

$$\boldsymbol{Z}_{t_{m+1}}(i) = \boldsymbol{Z}_{t_m}(i) + \boldsymbol{Y}_{t_m}(P(i)), \qquad i = 1, \dots, N.$$

The increment vectors $\boldsymbol{Y}_{t_m}$ are constructed from a suitable low discrepancy sequence $\boldsymbol{u}_1, \boldsymbol{u}_2, \boldsymbol{u}_3, \dots$ according to the rule

$$\boldsymbol{Y}_{t_m}(i) = \sqrt{h}\boldsymbol{H}^{-1}(\boldsymbol{u}_{mN+i})$$

where $\boldsymbol{H}(\boldsymbol{z}) = (H(z_1), \dots, H(z_s))$ with H given by

$$H(x) := \frac{1}{2}\left(1 + \operatorname{erf}\left(\frac{x}{\sqrt{2}}\right)\right) \quad \text{where} \quad \operatorname{erf}(z) = \frac{2}{\sqrt{\pi}}\int_0^z e^{-t^2} dt.$$

This construction ensures that the increments are properly distributed according to (13) and that the condition (15) can be met with $\boldsymbol{Y}_{t_m}$ in place of X_1 (for example, when $(\boldsymbol{u}_k)$ is a Faure sequence). As a consequence, the points $\boldsymbol{Z}_{t_m}$ play the role of X_2, so that a renumbering of these points is required to ensure a reasonable approximation of the product measure. This renumbering in the form of a permutation $P^{-1} : \{1, \dots, N\} \to \{1, \dots, N\}$ can be constructed by various sorting and mixing procedures based on the components of $\boldsymbol{Z}_{t_m}$. The resulting pairs $(\boldsymbol{Z}_{t_m}(P^{-1}(i)), \boldsymbol{Y}_{t_m}(i))$, or equivalently $(\boldsymbol{Z}_{t_m}(i), \boldsymbol{Y}_{t_m}(P(i)))$ are then used to define $\boldsymbol{Z}_{t_{m+1}}$ recursively. In [14], a family of algorithms (denoted QMC(m, r)) has been introduced which differ only in the construction of the permutation P. For example, QMC$(0, r)$ is based on a permutation which is constructed by sorting the components of $\boldsymbol{Z}_{t_m}(i)$ with respect to a bin-structure in the subspace of the first r coordinates. In the algorithm QMC$(m, 0)$, the sequence $\boldsymbol{u}_1, \boldsymbol{u}_2, \dots$ of uniformly distributed quasi random numbers is taken $(s+m)$-dimensional instead of s-dimensional, where the first s components are used to define $\boldsymbol{Y}_{t_m}$ and the last m components are taken to mix $\boldsymbol{Z}_{t_m}(i), \boldsymbol{Y}_{t_m}(i)$ in a quasi-random way (for details see [14]). Finally, QMC(m, r) represents the algorithm where both mixing and sorting is performed. The specific case with maximal values for m, r, i.e. QMC(s, s), is the algorithm proposed in [6]. The higher the values for m, r, the more expensive the construction of the permutation. Moreover, high values of m, r restrict the applicability in high dimensions because of hardware limitations. Therefore, it is important to check whether the algorithms with small m, r work satisfactorily.

For a numerical investigation, we consider the diffusion equation (8) with initial value $u_0(\boldsymbol{z}) = \pi^{-s/2}\exp(-|\boldsymbol{z}|^2)$. The exact solution for this problem is

$$u(\boldsymbol{z},t) = \frac{1}{(\pi(1+2t))^{s/2}}\exp\left(-\frac{|\boldsymbol{z}|^2}{1+2t}\right), \qquad \boldsymbol{z}\in\mathbb{R}^s. \tag{16}$$

Since the discrepancy between the point measure $\Pi_{\boldsymbol{Z}_{t_m}}$ associated to the approximate solution and the exact measure $u(t_m,\boldsymbol{z})d\boldsymbol{z}$ is difficult to compute exactly, we use the following approximation. Instead of comparing the two measures on *all* s-dimensional intervals of the form $(-\boldsymbol{\infty},\boldsymbol{\omega})$, we only choose a large number (10000) of such intervals where $\boldsymbol{\omega}$ is normally distributed with mean 3 and variance 1. Based on this error measure, we compute numerical convergence rates. For various methods mentioned above, we calculate the numerical convergence rate for different dimensions taking 100 time steps with $h = 0.0001$. The results are given in table 1. The Method MC refers to the Euler Maruyama method introduced in section 2 From table 1, we conclude

Table 1. Numerical order of convergence for the various methods. NA refers to non applicability due to memory restrictions.

Method	$s=3$	$s=6$	$s=9$	$s=12$	$s=50$
MC	-0.2698	-0.2538	-0.2862	-0.2765	-0.2946
QMC$(1,1)$	-0.4517	-0.4162	-0.5299	-0.4757	-0.6106
QMC$(0,1)$	-0.5662	-0.5407	-0.5783	-0.5542	-0.6070
QMC$(1,0)$	-0.00002	-0.0002	-0.0001	-0.0001	-0.00008
QMC(s,s)	-0.4555	NA	NA	NA	NA
QMC$(0,s)$	-0.2149	NA	NA	NA	NA
QMC$(s,0)$	-0.1715	NA	NA	NA	NA
QMC$(3,2)$	-0.1699	-0.4100	-0.2268	-0.4627	NA

that algorithm QMC$(0,1)$ outperforms the others. One can also observe that algorithm QMC$(1,1)$ performs well with the only disadvantage of extra mixing time. Algorithm QMC$(1,0)$ does not converge at all implying that sorting is essential for convergence and is in accordance with [7]. We stress that the numerical order of convergence is only one indication for the performance of the algorithm but one should also consider the absolute errors. Typical error plots corresponding to the results presented in table 1 are shown in figures 4 and 5. In conclusion, we can say that the methods QMC$(0,1)$ and QMC$(1,1)$ seem to be interesting alternatives for the Monte Carlo approach. Of course, the construction of the required permutation requires additional

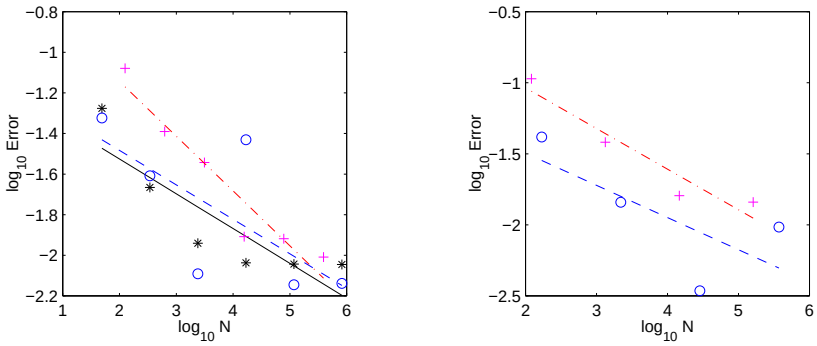

Figure 4. Even though the methods QMC$(s,0)$ (stars), QMC$(3,2)$ (circles) show a poor convergence order compared to the MC method (plus), the absolute error is still lower for particle numbers N below 10^6. The results are shown for dimensions $s=3$ (left) and $s=9$ (right). The convergence order is obtained as the slope of the least squares fit: solid line for QMC$(s,0)$, dashed line for QMC$(3,2)$, and dashed dot line for MC.

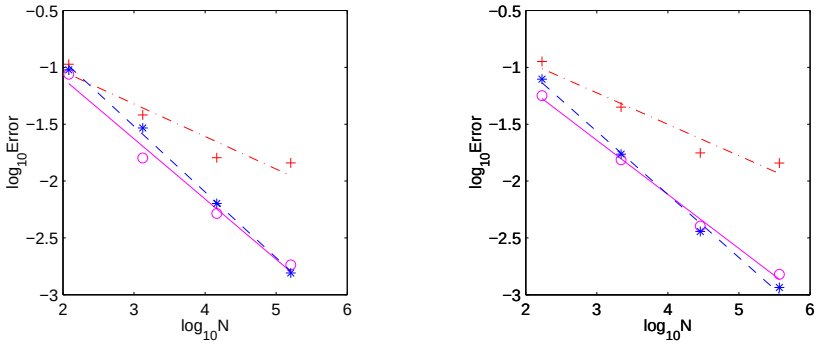

Figure 5. The methods QMC$(1,1)$ (circles) and QMC$(0,1)$ (stars) clearly outperform the Monte Carlo method both in convergence order and in absolute error. The left plot refers to dimension $s=9$ and the right one to $s=12$.

computational time but the increased accuracy allows to use lower particle numbers which balances this disadvantage.

4.2 The polymer model

Based on the previous considerations, we are able to construct approximate solutions of the polymer problem (5). The QMC algorithm has the form

$$\boldsymbol{Q}_{t_{m+1}}(i) = \boldsymbol{Q}_{t_m}(i) + \boldsymbol{a}(\boldsymbol{Q}_{t_m})h + D\boldsymbol{Y}_{t_m}(P(i)), \qquad i = 1,\ldots,N.$$

where the increments $\boldsymbol{Y}_{t_m}$ are defined as specified in the previous section. The permutation P is constructed according to the algorithm QMC$(1,1)$. As initial configuration distribution ψ_0, we compare three different choices

- (SN) $\psi_0(\boldsymbol{q}) = (2\pi)^{-s/2} \exp(-|\boldsymbol{q}|^2/2)$
- (DD) $\psi_0(\boldsymbol{q}) = \delta_{\boldsymbol{0}}(\boldsymbol{q})$
- (EQ) $\psi_0(\boldsymbol{q}) = N_{eq} \exp(-\phi(\boldsymbol{q}))$, with ϕ as in (1) (refer [2]).

The abbreviations SN, DD and EQ stand for standard normal, Dirac delta and equilibrium distribution respectively. As a result of the simulation, we consider a component of the integral functional $\boldsymbol{\tau}(t)$ defined in (6), where we replace the exact measure $\psi(t_m, \boldsymbol{q})\, d\boldsymbol{q}$ by the approximate point measure $\Pi_{\boldsymbol{Q}_{t_m}}$. A typical time evolution is shown in figure 6. If we focus on the sta-

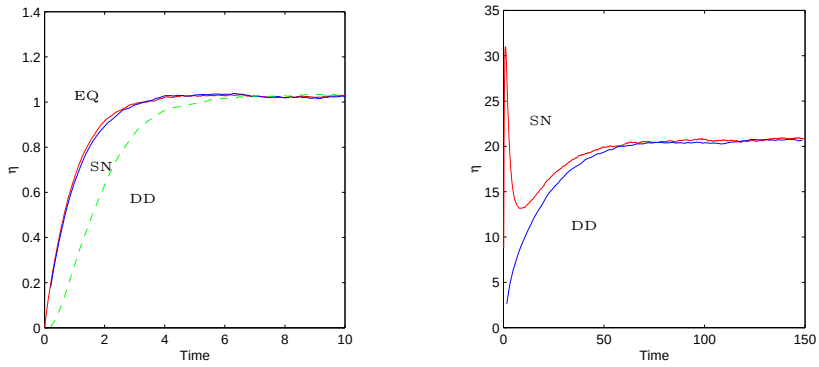

Figure 6. One component η of the functional $\boldsymbol{\tau}(t)$ for different choices of the initial condition. Left: the case of two beads $s = 3$ with $z = 0.1$, $\beta = 1.0$ and $d = 0.5$. Right: the case of eight beads $s = 21$ with the same force parameters. Obviously, the physically relevant stationary value is not influenced by the choice of the initial value.

tionary part of the curve which yields the required stationary value $\boldsymbol{\tau}^p$ defined in (3), we see that the result is noisy with a variation of the order of a few percent of the stationary value. The noise clearly reduces if we choose more particles (see figure 7). Compared to the MC result, the QMC algorithm shows considerably less oscillations. This can be seen in figure 8 where we compare the results of the algorithms for large t. It is clear that the QMC trajectory has less oscillations compared to the MC trajectory, meaning that one has to average MC over several runs to obtain a similar result. The average values obtained from the three separate runs of MC is shown in figure 8 (right). At this stage, we have the following situation: MC and QMC both work for high dimensions, the former can be implemented in a straightforward manner whereas the latter requires sorting the particle positions at each time step.

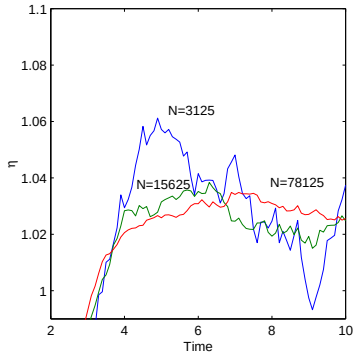

Figure 7. Variation of the component η of $\boldsymbol{\tau}(t)$ for large t decreases with increasing particle number. We indicate the case $s = 3$ with $z = 0.1$, $\beta = 1.0$ and $d = 0.5$.

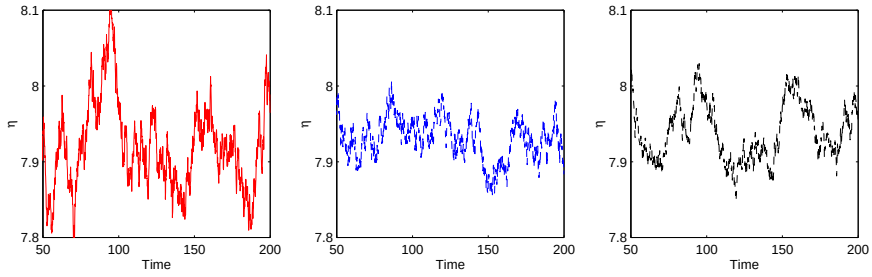

Figure 8. Component of $\boldsymbol{\tau}(t)$ with a single run of MC (left), QMC$(1, 1)$ (middle) and the average of three separate MC simulations (right) for the case of five beads $s = 12$ using 28561 particles with $z = 0.1$, $\beta = 1.0$ and $d = 1.0$.

The advantage with QMC is that the results have less noise compared to MC, but the extra processes required to properly represent the diffusion take up additional time. For the polymer problem, however, this does not contribute significantly as the evaluation of the function $\boldsymbol{a}(\boldsymbol{q})$ dominates the total computational time and this is required in both MC and QMC simulations. For further comparisons, we refer to [13].

References

1. R. Byron Bird, Charles. F. Curtiss, Robert. C. Armstrong, and Ole Hassager, *Dynamics of polymeric liquids*, vol. 1, Wiley Interscience, 1987.
2. _____, *Dynamics of polymeric liquids*, vol. 2, Wiley Interscience, 1987.
3. H. Faure, *Discrépance de suites associées à un systéme de numération (en dimension s)*, Acta Arith. **42** (1982), 337–351.
4. M. Junk and G. Venkiteswaran, *Constructing product measures with Quasi-Monte Carlo points*, preprint.

5. E. Kloeden and E. Platen, *Numerical solution of stochastic differential equations*, Springer, 1999.
6. C. Lécot and F. E. Khettabi, *Quasi-Monte Carlo simulation of diffusion*, Journal of Complexity **15** (1999), 342–359.
7. W. J. Morokoff and R. E. Caflisch, *A quasi-Monte Carlo approach to particle simulation of the heat equation*, Siam J. Numer. Anal. **30** (1993), no. 6, 1558–1573.
8. H. Niederreiter, *Random number generation and quasi-Monte Carlo methods*, vol. 6, Society for Industrial and Applied Mathematics, 1992.
9. E. Novak and K. Ritter, *The curse of dimension and a universal method for numerical integration*, Multivariate approximation and splines (G. Nüneberger, J.W. Schmidt, and G. Walz, eds.), ISNM, 1997, pp. 177–188.
10. H. C. Öttinger, *Stochastic processes in polymeric fluids*, Springer, 1996.
11. I. M. Sobol, *On the distribution of points in a cube and the approximate evaluation of integrals*, USSR Comput. Math. Math. Phys (1967).
12. G. Venkiteswaran, *A particle method for Fokker-Planck equations in high dimensions*, PhD dissertation, University of Kaiserslautern, Department of Mathematics, January 2003.
13. G. Venkiteswaran and M. Junk, *A QMC approach for high dimensional Fokker-Planck equations modelling polymeric liquids*, Math. Comp. Simul. **68** (2005), 23–41.
14. _____, *Quasi-Monte Carlo algorithms for diffusion equations in high dimensions*, Math. Comp. Simul. **68** (2005), 43–56.